Canted coupling of buried magnetic multilayers

V. Chakarian* and Y. U. Idzerda
Naval Research Laboratory, Code 6345, Washington, D.C. 20375

H.-J. Lin
AT&T Bell Laboratories, 600 Mountain Avenue, Murray Hill, New Jersey 07974

C. Gutierrez
Department of Physics, South West Texas State University, San Marcos, Texas 78666

G. A. Prinz
Naval Research Laboratory, Code 6345, Washington, D.C. 20375

G. Meigs and C. T. Chen
AT&T Bell Laboratories, 600 Mountain Avenue, Murray Hill, New Jersey 07974
(Received 12 October 1995)

Soft-x-ray magnetic circular dichroism is used as an element-specific magnetometer to determine the magnetic behavior of a buried 4.3 monolayer Mn film in a $Fe_{25}Co_{75}/Mn/Fe_{25}Co_{75}$ trilayer, which exhibits a 90° coupling between the two ferromagnetic films. By measuring element-specific magnetic hysteresis curves for Fe, Co, and Mn along directions parallel and perpendicular to an applied magnetic field, the magnetization behavior of each element is described, indicating an anomalous in-plane canting of the net Mn moment with respect to the Fe and Co moments by 23°.

The properties of buried and embedded layers, whether covered by a passivation layer or simply a component in a heterostructure, are often device defining. The task of studying these strategic layers becomes much more difficult when the measurement signal associated with the embedded layer is much smaller than the concurrent signal of the embedding media. Magnetic investigations of heteromagnetic multilayers are representative of this class of problem. Ferromagnet/metal/ferromagnet trilayers and superlattices exhibit exciting and technologically useful properties which are mainly defined by the interlayer.[1] The prototypical system is Fe/Cr/Fe which first demonstrated interlayer coupling[2,3] and giant magnetoresistance,[4] and continues to yield new developments. (For a review of the Fe/Cr/Fe system, see Ref. 5.) The overall magnetic behavior of these types of trilayers is predicted to be controlled to a large extent by the interlayer properties,[6] motivating a variety of studies to focus on the magnetic structure of simple overlayers of the interlying material as a starting point to understanding the trilayer coupling.[7–10]

Recently a new multilayer system, essentially bcc Co/Mn/Co (the actual composition of the trilayer is $Fe_{25}Co_{75}/Mn/Fe_{25}Co_{75}$), has been found to have quite a unique coupling behavior,[11] consistent with a recent theoretical model for systems with an ordered antiferromagnetic interlayer.[12] Instead of simply exhibiting aligned or antialigned configuration of the two ferromagnetic films, the results of magnetometry, ferromagnetic resonance,[11] and neutron scattering studies[13] of these trilayers indicate the magnetic moments of the two single-crystal FeCo alloy layers are strongly coupled at a fixed angle with respect to one another, requiring a very large magnetic field (15–20 kG) to overcome this coupling. Because this coupling angle is dependent on the thickness and perhaps roughness of the Mn layer, this unique magnetic configuration of the two alloy films must be reflected in an atypical magnetic structure of the embedded Mn layer.

Although these earlier works have described the magnetic behavior of the ferromagnetic FeCo alloy films, no experimental determination of the magnetic structure of the interlayer Mn, the central mechanism of the coupling, was made. To establish the magnetic structure of the buried Mn layer by conventional magnetic characterization techniques is not possible because the magnetic signatures of the FeCo alloy layers are 2–3 orders of magnitude larger than the signature of the Mn film. Perhaps the only method which is capable of separating the magnetic Mn signal from those of the Fe and Co is soft-x-ray magnetic circular dichroism (MCD), an element-specific magnetic spectroscopic tool where the difference in the absorption of left- and right-circular polarized photons is measured at the absorption edges of the constituent elements. Soft-x-ray MCD is capable of determining the magnetic order of overlayers[10,14,15] and buried layers[16] with high sensitivity. MCD measurements made in an applied magnetic field can be used to generate element-specific magnetic hysteresis curves which in turn can be used to dissect complicated total-moment hysteresis curves into their elemental components,[17] extract magnetoresistance values independent of multidomain and incomplete moment alignment effects,[18] and can even be used as an element-specific magnetometer (ESM),[19] where all three components of the magnetic moment vector are determined for each element or layer.

In this Brief Report, by using the ESM technique, we demonstrate that surprisingly, the Mn interlayer possesses a

 © 1996 The American Physical Society

net magnetic moment which exhibits a nearly field-independent *canting* of 23° relative to the average moments of Fe and Co. From the evolution of these moments in response to an arbitrary applied field, a detailed description of Mn magnetization behavior can be constructed to help understand the unique coupling found in this system.

The magnetic multilayer, representative of the 15 different trilayers generated, consists of two single crystal 100 Å $Fe_{25}Co_{75}$ alloy films[20] deposited at 175 °C, separated by a thin 4.3 monolayer (ML) (8.7 Å) Mn interlayer grown below room temperature (0 °C) to minimize Mn clustering. The trilayer was grown on a thick ~660 Å ZnSe(001) buffer layer and capped with a 30 Å Al film to prevent oxidation.[11] Although these trilayers display a distribution of coupling angles between the two high quality FeCo alloy films, this trilayer structure displays both a large Mn MCD signal and a coupling angle of ~90°.

The ESM experiments were conducted at the NRL/NSLS U4B beamline located at the National Synchrotron Light Source.[21–23] The element-specific magnetic hysteresis curves were determined by monitoring the partial x-ray fluorescence yield, as a function of the applied magnetic field, at the L_3 edges of the relevant elements.[17] A liquid-nitrogen cooled electromagnet capable of reaching ~3 kG is mounted with the sample placed between its poles such that the applied magnetic field is parallel to the sample surface. The samples were kept at room temperature and the incidence angle of the incoming photon beam, θ, was fixed at 60° from the surface normal with a degree of circular polarization of 75%.

The ESM studies of the Fe, Co, and Mn showed that each film of the trilayer exhibits *only* an in-plane magnetization, i.e., $\mathbf{M}=M_x\hat{\mathbf{x}}+M_y\hat{\mathbf{y}}$ at all applied fields directed along the x axis. Briefly,[19] in order to determine the M_x and M_y components of $\mathbf{M}$, the intensity of the L_3 absorption peak was measured as a function of magnetic field for circularly polarized photon beam directions in the $x-z$ and $y-z$ planes of the sample (as indicated by $\mathbf{k}_1$ and $\mathbf{k}_2$ in the inset of Fig. 1; z direction defined along surface normal) and at 45° to these two planes. The former two orientations yield the M_x and M_y hysteresis curves (since $M_z=0$), while the latter yields $(M_x+M_y)/\sqrt{2}$ and serves as an internal normalization of the M_x and M_y curves. The lack of an M_z component was verified directly by measuring a null MCD signal for photon beam incident normal to the film plane.

Although our intent is to study the magnetic behavior of the Mn interlayer, comparison to the behavior of the ferromagnetic layers will prove to be instructive. In Fig. 1, the relative M_x and M_y magnetization curves for Fe are shown. The magnetic field, which is always applied along the $\langle 110\rangle$ direction (x axis), is varied between ± 2.2 kOe. These normalized curves were obtained in less than 3 h and have been corrected for the small saturation effects.[24] The larger concentration of Co requires larger saturation effect corrections, therefore, the Co magnetization curves, although identical to the Fe curves, were not used. Note that, due to large probing depth of the fluorescence yield measurements, the Fe magnetization curves shown in Fig. 1 represent the response of the *average* $\mathbf{M}$, $\langle\mathbf{M}\rangle_{\mathrm{Fe}}$, of the Fe in both FeCo films which are coupled at 90° to each other, and not the individual moments of a single film. As the field intensity is reduced, the average Fe moment in the x direction,

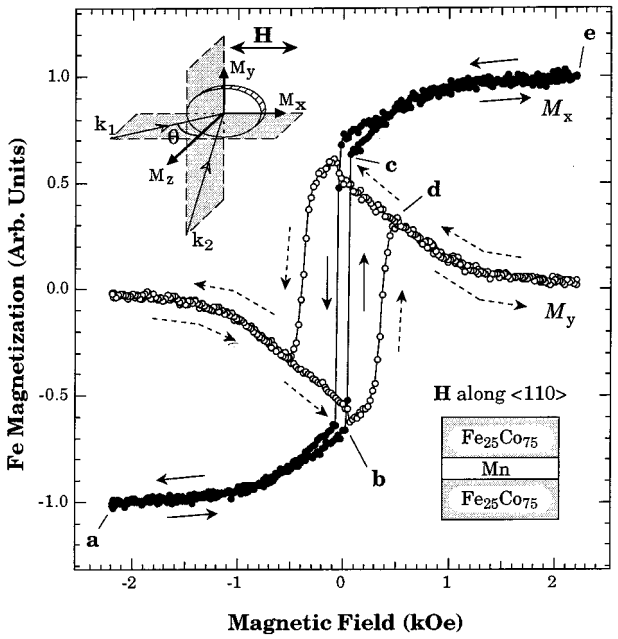

FIG. 1. M_x and M_y hysteresis loops for Fe where the points are the data and the solid curves are provided as a guide to the eye. The arrows indicate increasing and decreasing magnetic field for the M_x (solid arrows) and M_y (dashed arrows) magnetization curves. Insets: measurement configurations for the determination of M_x and M_y and a schematic view of the trilayer.

$\langle M_x\rangle_{\mathrm{Fe}}$, shows a gradual reversible decrease while $\langle M_y\rangle_{\mathrm{Fe}}$ increases indicating a near coherent rotation of the magnetization vector away from the applied field direction. The $\langle M_x\rangle_{\mathrm{Fe}}$ curve displays a single, irreversible transition (from b to c) at the critical fields of ± 55 Oe. The intensity of $\langle M_y\rangle_{\mathrm{Fe}}$, on the other hand, is nearly unchanged during the abrupt change in $\langle M_x\rangle_{\mathrm{Fe}}$, and displays a decidedly less abrupt transition beginning at ± 100 Oe.

These two interdependent hysteresis loops can be combined to form a single two-dimensional (2D) parametric representation of $\langle\mathbf{M}\rangle_{\mathrm{Fe}}$, shown in Fig. 2. This 2D representation can be superimposed on the principal crystallographic directions of the surface to create an accurate portrayal of $\langle\mathbf{M}\rangle_{\mathrm{Fe}}$, both in magnitude and direction. As the magnetic field is scanned from -2.2 kOe to $+2.2$ kOe, $\langle\mathbf{M}\rangle_{\mathrm{Fe}}$ traverses the lower half of the loop in the counter-clockwise (ccw) direction, as indicated by the arrows. For the opposite field variation, $\langle\mathbf{M}\rangle_{\mathrm{Fe}}$ traverses the upper half of the loop. Several positions on the loop have been marked with letter symbols which correspond to the points on Fig. 1 with the same labeling letter.

By taking the 90° coupling between the two FeCo films into account, the 2D parametric loop can be used to model the behavior of the magnetic moments of each FeCo layer as a function of the applied field (shown above Fig. 2). At the maximum applied fields, the average moment is aligned with the field direction, but since the field is far smaller than the coupling strength, the two individual films are each oriented $\pm 45°$ to the applied field (point a). As the field intensity is reduced, but prior to its reversing sign, the two individual moments move away from the $\langle 100\rangle$ directions toward the $\langle 110\rangle$ directions (point b) indicating that, for the individual

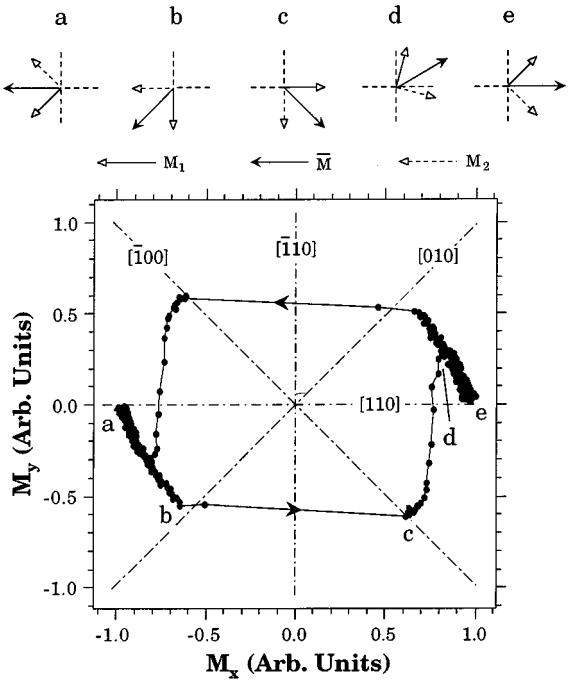

FIG. 2. 2D parametric representation of average Fe moment generated from the data of Fig. 1. Also shown above the figure is a vector model describing the moment reversal process.

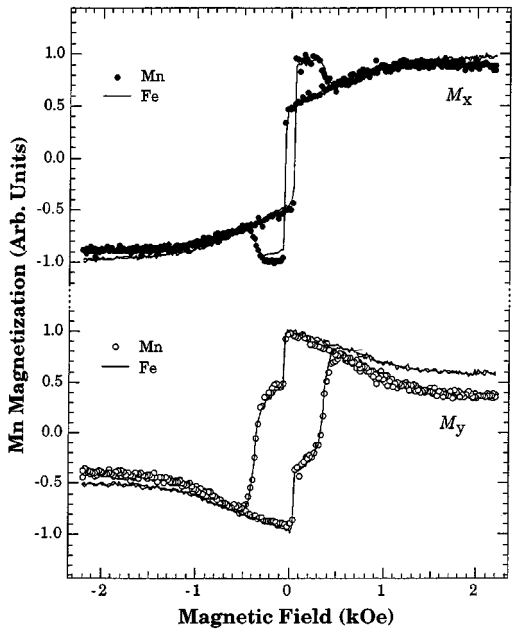

FIG. 3. M_x and M_y hysteresis loops for Mn (points). The solid curves are the corresponding Fe loops generated by the inclusion of a rotation of 23° to the data of Fig. 1.

films, the $\langle 110 \rangle$ axes are magnetically easy. The magnetic configuration of the two films abruptly changes by 90° so that, for two films of nearly equal thickness, the y component of the average magnetization is nearly conserved while the x component changes sign. Unlike the nearly coherent rotation of the magnetization vectors in going from point a to point b, the transition from point b to point c is accomplished by the formation and coalescence of magnetic domains, clearly expressed by the overall loss in magnitude of the average magnetization vector.

As the field is further increased, a second, decidedly less abrupt transition occurs, again, mediated by domain dynamics. In this case the domain coalescence is quite slow, occurring over a large field range (c to d), and a simultaneous rotation of the average moment toward the applied field direction occurs (point d). A further field increase results in a continued magnetization rotation until alignment with the applied field is accomplished (point e). As the field is swept in the opposite direction, the magnetization process is not reversed (i.e., a clockwise rotation), but rather $\mathbf{M}_1$ and $\mathbf{M}_2$ continue this ccw rotational scheme due to a growth induced uniaxial magnetic anisotropy which makes one crystallographic axis preferred.[19,20] To assure that this ccw rotation was not due to a experimental artifacts, e.g., sample and/or magnetic field misalignments, the measurements were repeated with the applied field at an angle of 10° away from the [110] direction in an attempt to *force* the moment rotation to reverse direction. The results were identical, experimentally confirming the presence of the uniaxial magnetic anisotropy.

It is interesting to contrast this behavior with that of the Mn magnetization, shown in Fig. 3. The fact that the Mn interlayer is hysteretic indicates that the Mn possesses a net ferromagnetic moment. This alone is quite unique because similar MCD measurements of Fe/Cr/Fe trilayers showed that the Cr interlayer had a completely antiferromagnetic structure and therefore no net moment.[10] The difference between the Cr and Mn magnetic behavior is all the more remarkable in that MCD studies of overlayers of Cr on bcc Fe(001) (Ref. 10) and overlayers of Mn on bcc Co(001) found identical overlayer behavior. For submonolayer coverage, the overlayer moments were antialigned to the substrate moment, and as the thickness of the overlayer was increased, the MCD signal was continually reduced. This is consistent with the bulk type-I antiferromagnetic ordering which, for the bcc (001) orientation, consists of alternating ferromagnetic sheets antialigned with the adjoining layers as is experimentally observed for the Cr(001) surface.[25,26] Due to the statistical roughness of the overlayer, for coverage >3 ML, this antiferromagnetic structure results in no *net* overlayer moment as measured by MCD. Although, there is no net moment for the Mn overlayer, the deposition of a second ferromagnetic layer reestablishes a *net* Mn moment within the trilayer film, indicating that although the Mn interlayer has an antiferromagnetic basis, its actual structure is not simple.

At first glance, the behavior of the Mn hysteresis loops (6 h of acquisition) seem much more complex than the Fe or Co loops, displaying multiple jumps in both the M_x and M_y magnetization. Only after constructing the 2D M_x vs M_y parametrized curve of the $\langle \mathbf{M} \rangle_{\mathrm{Mn}}$ and superimposing that of the $\langle \mathbf{M} \rangle_{\mathrm{Fe}}$ (shown in Fig. 4) do we recognize that the seemingly complicated Mn hysteresis loops are the result of a nearly rigid 23° rotation of $\langle \mathbf{M} \rangle_{\mathrm{Mn}}$ with respect to $\langle \mathbf{M} \rangle_{\mathrm{Fe}}$. This rotation is most clearly demonstrated in Fig. 3 when we overlay the Mn data (shown as the dots) with the Fe M_x and M_y data after a rotation of 23° (solid line). All the elements of the magnetization behavior of the Mn are reproduced by the Fe spectra (with the inclusion of the rotation). The rotation angle, however, is not completely field independent and

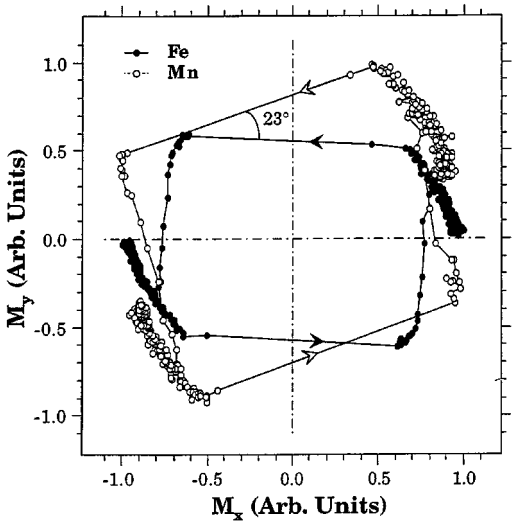

FIG. 4. 2D parametric representations of $\langle \mathbf{M} \rangle_{\mathrm{Fe}}$ and $\langle \mathbf{M} \rangle_{\mathrm{Mn}}$ clearly showing the canting of $\langle \mathbf{M} \rangle_{\mathrm{Mn}}$ with respect to $\langle \mathbf{M} \rangle_{\mathrm{Fe}}$.

varies from 25° at low fields to only 21° at high fields. The 23° rotation is inconsistent with an interdiffusion of the Mn into the FeCo alloy layers. Such an interdiffusion results in an antialigned (180°) Mn moment to that of Fe (Co).

Both the presence of a net Mn moment and its rotation from the net Fe moment can be understood if the microscopic magnetic structure of the Mn interlayer is an antiferromagnetic helix structure, consistent with the proposed helical structure for a system with an ordered antiferromagnetic interlayer bounded by ferromagnetic sheets.[12] This structure is similar to the bulk antiferromagnetic ordering for the bcc(001) orientation described earlier but with the added feature of a slight rotation of the magnetic moment of each adjacent antialigned Mn layer, forming a helix. The first Mn layer is slightly rotated from being antialigned to the first Fe (Co) moment direction. The second Mn layer is antialigned and slightly rotated ($180 \pm \delta\theta$) from the first Mn layer. This canting continues through the Mn layers until the last layer is only slightly rotated away from the second Fe (Co) moment direction, which is at 90° with respect to the first. Because of this rotation, the magnetic moment of each Mn layer is not completely compensated for by the moment of the subsequent Mn layer (as occurs in the bulk antiferromagnetic structure) resulting in a residual net Mn moment with an overall rotation with respect to the net Fe moment of the two FeCo films.

If the trilayer structure is symmetric (equal roughness at both interfaces), this simple model would predict a symmetric distribution of Mn moment directions for the Mn layers and cannot predict a residual Mn moment at 23° from the net Fe moment. But a realistic description of the structure of the trilayer must account for the nonintegral number of Mn layers and the different degrees of roughness present in the two Mn/FeCo interfaces (the second Mn interfaces are much rougher than the first). As an approximation, the trilayer can be straightforwardly modeled with a smooth Mn interface followed by a rough Mn interface, with an average of a total of 4.5 layers of interlying Mn. This asymmetric structure results in a net Mn moment with a direction dependent on the actual distribution of Mn thicknesses. Choosing a realistic distribution of thicknesses (generated from a Poisson distribution which is accurate if no diffusion of the Mn occurs) a canting angle of 23° of the net Mn moment direction from the net Fe moment direction can be obtained. Furthermore, this helical model predicts that as the coupling angle of the two enclosing ferromagnetic films is decreased (at higher applied fields), the net Mn moment would both be reduced in its magnitude and its rotation angle, as is experimentally observed. Other micromagnetic descriptions of the Mn interlayer can be proposed (ferrimagnetic Mn clusters, layer dependent Mn moment, etc.), but they must be consistent with the observed hysteretic behavior found here.

One of the authors (V.C.) was supported by the Office of Naval Research. Work done at National Synchrotron Light Source was supported by DOE, under Contract No. DE-AC02-76CH00016.

*Mailing address: NSLS Bldg. 725A/U4B, Brookhaven National Laboratory, Upton, NY 11973.

[1] L. M. Falicov *et al.*, J. Mater. Res. **5**, 1299 (1990).
[2] P. Grünberg, J. Appl. Phys. **57**, 3673 (1985).
[3] P. Grünberg *et al.*, Phys. Rev. Lett. **57**, 2442 (1986).
[4] M. N. Baibich *et al.*, Phys. Rev. Lett. **61**, 2472 (1988).
[5] B. Heinrich and J. F. Cochran, Adv. Phys. **42**, 523 (1993).
[6] J. C. Slonczewski, Phys. Rev. Lett. **67**, 3172 (1991).
[7] R. Jungblut *et al.*, J. Appl. Phys. **70**, 5923 (1991).
[8] J. Unguris *et al.*, Phys. Rev. Lett. **69**, 1125 (1992).
[9] T. G. Walker *et al.*, Phys. Rev. Lett. **69**, 1121 (1992).
[10] Y. U. Idzerda *et al.*, Phys. Rev. B **48**, 4144 (1993).
[11] M. E. Filipkowski *et al.*, Phys. Rev. Lett. **75**, 1847 (1995).
[12] J. C. Slonczewski, J. Magn. Magn. Mater. **150**, 13 (1995).
[13] J. F. Ankner *et al.* (unpublished).
[14] J. H. Tjeng *et al.*, J. Magn. Magn. Mater. **109**, 288 (1992).
[15] J. G. Tobin *et al.*, Phys. Rev. Lett. **68**, 3642 (1992).
[16] Y. Wu *et al.*, Phys. Rev. Lett. **69**, 2307 (1992).
[17] C. T. Chen *et al.*, Phys. Rev. B **48**, 642 (1993).
[18] Y. U. Idzerda *et al.*, Appl. Phys. Lett. **64**, 3503 (1994).
[19] V. Chakarian *et al.*, Appl. Phys. Lett. **66**, 3368 (1995).
[20] C. J. Gutierrez *et al.*, J. Appl. Phys. **61**, 2476 (1992).
[21] C. T. Chen and F. Sette, Rev. Sci. Instrum. **60**, 1616 (1989).
[22] C. T. Chen, Rev. Sci. Instrum. **63**, 1229 (1992).
[23] C. T. Chen *et al.*, Phys. Rev. B **42**, 7262 (1990).
[24] Y. U. Idzerda *et al.*, Nucl. Instrum. Methods Phys. Res. A **347**, 134 (1994).
[25] L. E. Klebanoff *et al.*, Phys. Rev. B **32**, 1997 (1985).
[26] R. Wiesendanger *et al.*, Phys. Rev. B **65**, 247 (1990).